

# Mitigating the Risk of Voltage Collapse using Statistical Measures from PMU Data

Samuel Chevalier, *Student Member, IEEE*, Paul D. Hines, *Senior Member, IEEE*

**Abstract**—With the continued deployment of synchronized Phasor Measurement Units (PMUs), high sample rate data are rapidly increasing the real time observability of power systems. Prior research has shown that the statistics of these data can provide useful information regarding network stability, but it is not yet known how this statistical information can be actionably used to improve power system stability. To address this issue, this paper presents a method that gauges and improves the voltage stability of a system using the statistics present in PMU data streams. Leveraging an analytical solver to determine a range of “critical” bus voltage variances, the presented methods monitor raw statistical data in an observable load pocket to determine when control actions are needed to mitigate the risk of voltage collapse. A simple reactive power controller is then implemented, which acts dynamically to maintain an acceptable voltage stability margin within the system. Time domain simulations on 3-bus and 39-bus test cases demonstrate that the resulting statistical controller can out-perform more conventional feedback control systems by maintaining voltage stability margins while loads simultaneously increase and fluctuate.

**Index Terms**—Synchronized phasor measurement units, voltage collapse, critical slowing down, holomorphic embedding, first passage processes

## I. INTRODUCTION

**I**N order to optimize the use of limited infrastructure, transmission systems frequently operate close to their stability or security limits. Although economically advantageous [1], this can lead to elevated blackout risk given the fluctuating nature of supply and demand [2]. Consequently, stability margin estimation is an essential tool for power system operators. Predicting the onset of voltage instability, though, is often made difficult by reactive support systems and tap changing transformers that hold voltage magnitudes high as load increases. Although voltage support is essential for reliable operations, these controls can sometimes hide the fact that a system is approaching a voltage stability limit, particularly when operators and control systems rely on voltage magnitude data for control decisions.

Across a variety of complex systems, there is increasing evidence that indicators of emerging critical transitions can be found in the statistics of state variable time series data [3]. Termed Critical Slowing Down (CSD) [4], this phenomenon most clearly appears as elevated variance and autocorrelation in time-series data [5]. More recently, CSD has been successfully investigated in the power systems literature, and strong

connections have been drawn between bifurcation theory and the elevation of certain statistics in voltage and current time series data [6]–[9]. In particular, [9] presents a method for analytically calculating the time series statistics associated with a stochastically forced dynamic power system model. We leverage these results to predict key statistics of a power system that is approaching a critical transition. Others, such as [10], have developed control methods that use voltage magnitude declination rate measurements, but do not explicitly use statistical information as we present in this paper.

As reviewed in [11], power systems are liable to experience a variety of critical transitions, including Hopf, pitchfork, and limit-induced bifurcations. This paper is primarily concerned with the slow load build up, reactive power shortages, and other Long Term Voltage Stability (LTVS) processes that may contribute to a Saddle-Node bifurcation of the algebraic power flow equations. Classic voltage stability, which refers to a power system’s ability to uphold steady voltage magnitudes at all network buses after experiencing a disturbance, is lost after a network experiences this sort of bifurcation [12]. The methods in this paper aim to preserve such voltage stability and thus prevent a system from experiencing voltage collapse.

The goal of this paper is to describe and evaluate a control system that uses the variance of bus voltages to reduce the probability of voltage collapse in a stochastic power system. This control system leverages a number of innovative tools to perform this task. The first uses the load scaling factor from the Holomorphic Embedding Load Flow Method (HELM) [13] to represent a slowly varying stochastic variable, such as changes in overall load levels over time. Second, a First Passage Process (FPP) [14] is used to identify critical loading thresholds given the statistics of the slower load changes. Finally, a full order dynamical system model is used to analytically predict the expected algebraic variable covariance matrix of the system, given stochastic load noise excitation, for the previously identified critical loading level. The associated critical variances from this matrix are then used as a reference signal to control a static VAR compensator (SVC). This reference signal is dynamically updated as network configurations change and equilibriums shift. In building this controller (see Fig. 8), we combine static algebraic voltage collapse analysis through HELM, the first passage probability, statistical estimation (based on system model and load noise assumptions) and network feedback in order to leverage the statistical properties of PMU data to reduce the risk of voltage instability.

The remainder of this paper is organized as follows. Section II motivates the use of voltage variance as an indicator of stability and presents the methods employed in our statistical

S. Chevalier is with the Department of Mechanical Engineering at the Massachusetts Institute of Technology, Cambridge, MA 02139 (e-mail: schev@mit.edu).

P.D.H. Hines is with the Dept. of Electrical and Biomedical Engineering at the University of Vermont, Burlington, VT 05405 USA (e-mail: paul.hines@uvm.edu).

controller. Section III describes the new statistical controller along with two conventional reactive power controllers that we use to benchmark our results against. Section IV demonstrates the statistical controller on a 3 bus power system consisting of a generator, a load bus, and an SVC bus. For further validation, Section V tests the controllers on the IEEE 39 bus system. Finally, conclusions and ideas for future research are presented in Section VI.

## II. BACKGROUND

This section motivates the use of bus voltage variance as a measure of stability and presents the methods and tools used to build our statistical controller.

### A. Bus Voltage Variance in a 2 Bus Power System

A variety of systems, such as capacitor banks, tap changing transformers, and various Flexible AC Transmission System (FACTS) devices, are employed in power systems to ensure that voltage magnitudes remain sufficiently high. As a result, voltage magnitudes are an imperfect indicator of the proximity of a system to its voltage stability limits. To understand how an overloaded system with high voltage magnitudes may have a compromised voltage stability margin, we begin with the definition in [15] (p.262): “For a particular operating point, the amount of additional load in a specific pattern of load increase that would cause a voltage collapse is called the loading margin.”

Consider the system in Fig. 1, where capacitive shunt support  $B_s$  and a constant power load  $P+jQ$  are placed at the “to” bus and a generator with fixed voltage is located at the “from” bus. Fig. 2 shows the power-voltage curves that result if the load’s power factor is held fixed with several different amounts of reactive power injection.

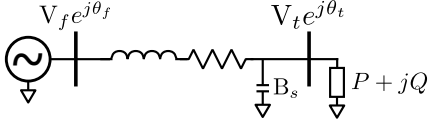


Fig. 1. Two Bus Model with Generator, Load and Shunt Capacitor  $B_s$

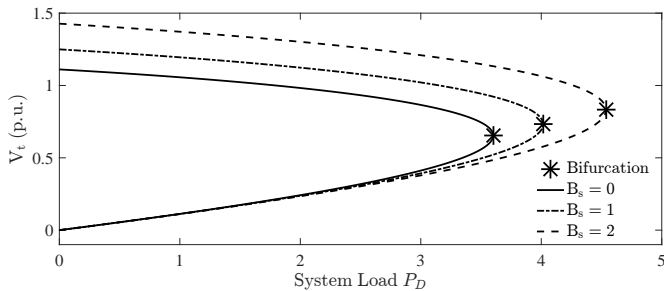


Fig. 2. Load Bus Voltage as a Function of  $P_D$  for Various Shunt Values. As more reactive power is injected into the system, the voltage magnitude at the point of bifurcation drifts upwards towards nominal system voltage.

As reactive support increases, the system can sustain larger increases in load before voltage collapse occurs. However, if reactive resources are used to maintain voltages at their

nominal levels (1 p.u.), the load margin to the bifurcation decreases (as seen by the upward drift of the star symbols). On the other hand, as load increases, the magnitude of the derivative of the PV curve (with respect to load) increases, suggesting that this derivative is a useful indicator of proximity to the bifurcation.

If load varies stochastically with variance  $\sigma_{P_D}^2$ , (1) describes the expected bus voltage variance at the load bus, given load noise  $\sigma_{P_D}^2$  and load level expected value  $E[P_D]$ :

$$\sigma_{V_t}^2 \approx \left( \frac{dV_t}{dP_D} \Big|_{E[P_D]} \right)^2 \sigma_{P_D}^2 \quad (1)$$

Predicting the distance to static voltage collapse with variance measurements can be accomplished by (i) drawing the PV curve for a system, (ii) defining a complex power loading margin on the curve which should not be exceeded, and then (iii) calculating the expected bus voltage variance at this threshold. If measured voltage variance exceeds this threshold value then the system may be at risk of exceeding its stability limits. If reactive support is high, the voltage magnitude of the system may be an unreliable real time measure of voltage stability. The bus voltage variance statistic, however, can potentially tell a more complete story about system stability. In the following sections, we leverage the stability information encoded in the variance in order to make real-time, data-driven control decisions.

### B. System Model Overview

As described in [9] a stochastically forced power system can be modeled with a set of Differential-Algebraic Equations (DAEs) [16] of the form

$$\dot{\mathbf{x}} = \mathbf{f}(\mathbf{x}, \mathbf{y}) \quad (2)$$

$$\mathbf{0} = \mathbf{g}(\mathbf{x}, \mathbf{y}, \mathbf{u}(t)) \quad (3)$$

where  $\mathbf{f}$ ,  $\mathbf{g}$  represent the differential and algebraic systems,  $\mathbf{x}$ ,  $\mathbf{y}$  are the differential and algebraic state variables, and  $\mathbf{u}(t)$  represents the time-varying stochastic (net) load fluctuations. Neglecting for the moment the slow changes in load level, the complex load at time  $t$  can be represented by (4):

$$\mathbf{S}(t) = \mathbf{S}_0(1 + \mathbf{u}(t)) \quad (4)$$

with the dynamics of the fast load fluctuations given by the Ornstein-Uhlenbeck process expressed in (5):

$$\dot{\mathbf{u}} = -E\mathbf{u} + I_n \xi \quad (5)$$

where  $I_n$  is the  $n \times n$  identity matrix and  $E$  is a diagonal matrix of inverse time correlations.  $\xi$  is a vector of zero-mean independent Gaussian random variables. We assume that a grid operator can estimate the statistics of load fluctuations ( $E$  and  $\xi$ ) from measurements.

### C. Computing the Algebraic Variable Covariance Matrix

The process for deriving the approximate covariance matrix for all variables in a stochastically forced power system is derived in [9]. This computation allows one to characterize the statistics of a system that is approaching a bifurcation. This

method is based on linearizing the equations encompassed by (2) and (3) and then algebraically solving for  $\Delta\dot{\mathbf{x}}$  and  $\Delta\dot{\mathbf{u}}$  by eliminating the algebraic variable vector  $\Delta\mathbf{y}$ .

$$\begin{bmatrix} \Delta\dot{\mathbf{x}} \\ \Delta\dot{\mathbf{u}} \end{bmatrix} = \begin{bmatrix} A_s & -\mathbf{f}_y \mathbf{g}_y^{-1} \mathbf{g}_u \\ 0 & -E \end{bmatrix} \begin{bmatrix} \Delta\mathbf{x} \\ \Delta\mathbf{u} \end{bmatrix} + \begin{bmatrix} 0 \\ I_n \end{bmatrix} \underline{\xi} \quad (6)$$

where  $A_s$  is the standard state matrix. Using  $\mathbf{z} = [\Delta\mathbf{x} \ \Delta\mathbf{u}]^T$ , (6) can be rewritten with compact matrices  $A$  and  $B$ .

$$\dot{\mathbf{z}} = A\mathbf{z} + B\underline{\xi} \quad (7)$$

As introduced in [17], the Lyapunov equation (8) can be solved numerically to calculate the covariance matrix of  $\mathbf{z}$ , where  $A$  and  $B$  are defined in (7).

$$A\sigma_z^2 + \sigma_z^2 A^T = -BB^T \quad (8)$$

Since  $\Delta\mathbf{y} = [-\mathbf{g}_y^{-1} \mathbf{g}_x \quad -\mathbf{g}_y^{-1} \mathbf{g}_u] \Delta\mathbf{z} = K\Delta\mathbf{z}$ , the state variable covariance matrix can be transformed into the algebraic variable covariance matrix  $\sigma_y^2 = K\sigma_z^2 K^T$ , and a subset of the diagonal entries of  $\sigma_y^2$  contain the bus voltage variances.

#### D. Adapting HELM to Solve CPF

The Continuation Power Flow (CPF) problem is a classic approach to understanding and predicting voltage instability. As outlined in [18], CPF involves drawing PV curves given load and generation increase rates using iterative Newton-Raphson methods. As introduced in [13], iterative techniques, such as Newton-Raphson, can encounter a numerical issues, such as divergence or finding undesirable low-voltage solutions, when solving the nonlinear power flow equations, particularly when a system approaches a Saddle-node bifurcation. An alternative is to use the Holomorphic Embedding Load-flow Method (HELM), which uses complex analysis and recursive techniques to overcome these numerical difficulties. If one exists, HELM is guaranteed to compute the high voltage power flow solution [19].

Prior work [20] provides an important foundation for using HELM to solve for the static stability margins of a power system. After generating the holomorphic voltage functions, the largest, positive zero of the numerator of the Padé approximant approximates the maximum power transfer point of the system. This method, though, scales all loads at uniform rates, and does not account for more than one single generator bus in the system. In order to solve these problems, we derive a new method for scaling loads from a known base case solution. This approach allows loads and generators to scale at different rates.

In the conventional CPF problem, generation participation rates are assigned to generators to pick up excess load as it is scaled. This is not the approach we took. For mathematical simplicity, we instead solve the base case power flow solution and then fix the generator voltage phase angles. As load increases at the load buses, generation throughout a system increases quasi-proportionally to the electrical distance between the generator and the load. Electrically proximal generators respond with the largest generation increases, while electrically distant generators respond with smaller increases; we justify these assumptions in [21]).

The details of the method are described in [21] and summarized in the following. We begin with the holomorphically embedded power flow equation at the  $i^{\text{th}}$  PQ bus.

$$\sum_{k=1}^N Y_{i,k} V_k(s) = \frac{S_i^* + sk_i S_i^*}{V_i^*(s^*)} \quad i \in \text{PQ} \quad (9)$$

In (9), the parameter  $k_i$ , which can be positive, negative, or 0, corresponds to the rate at which bus  $i$  will be loaded. If  $k_i = 0$ , the load at bus  $i$  will not change as the overall loading rate  $s$  increases from 0. The holomorphically embedded equations at voltage controlled buses (PV and reference) are stated:

$$V_i(s) = V_i e^{j\theta_i} \quad i \in \{\text{PV} \cup \text{r}\} \quad (10)$$

Generator voltages are independent of  $s$  (reactive power limits are not considered). Once the power series coefficients of the holomorphic voltage functions  $V_i(s)$  have been calculated via  $N_c$  recursive routines, Padé approximants ( $A$  and  $B$  in (11)) are evaluated at various values of  $s$  in order to compute the complex voltages at each bus.

$$\sum_{n=0}^{N_c-1} V[n](s^n) = \frac{\sum_{n=0}^{\frac{N_c-1}{2}} A[n](s^n)}{\sum_{n=0}^{\frac{N_c-1}{2}} B[n](s^n)}, \quad N_c \text{ odd} \quad (11)$$

In order to validate this continuation method, which we refer to as *CPF via HELM*, we test our method on the IEEE 39 bus system. We first define the vector  $\mathbf{k}$  which has length 39. The elements of this vector contain the respective arbitrary loading rates of the buses in the system.

$$\mathbf{k}_i = \begin{cases} 1 & i \in \{3, 4, 7, 8\} \\ -0.2 & i = 20 \\ 0 & \text{otherwise} \end{cases} \quad (12)$$

The loads of the system scale in the following way, where  $S_i^0$  is the base load at bus  $i$  in the system:  $S_i = S_i^0 + sk_i S_i^0$ . In this example, we scale  $s$  from 0 to 1.99, at which point the Saddle-Node Bifurcation occurs. Once the Padé approximants are known for each bus, we scale  $s$  and solve for the complex voltages at each bus. The resulting PV curves are shown in Panel (a) of Figure 3.

We also validated HELM against conventional Newton Raphson Power Flow (NRPF). As  $s$  was increased and the load was scaled via HELM, we solved for load bus voltages using NRPF. We then plotted the difference between the HELM and the NRPF voltage magnitudes in panel (b). These results suggest that *CPF via HELM* accurately computes load bus phasor voltages for a given level of load increase.

#### E. Deriving a Probabilistic Loading Margin from First Passage Processes

CPF (via HELM or NRPF) allows one to estimate how much margin exists between the current operating point and voltage instability. However, it does not tell the chance of a particular system coming dangerously close to the point of instability. This section builds on the First Passage Process literature to systematically compute the probability that load will not increase beyond a collapse threshold during a given time period. To do so, we model the holomorphic parameter

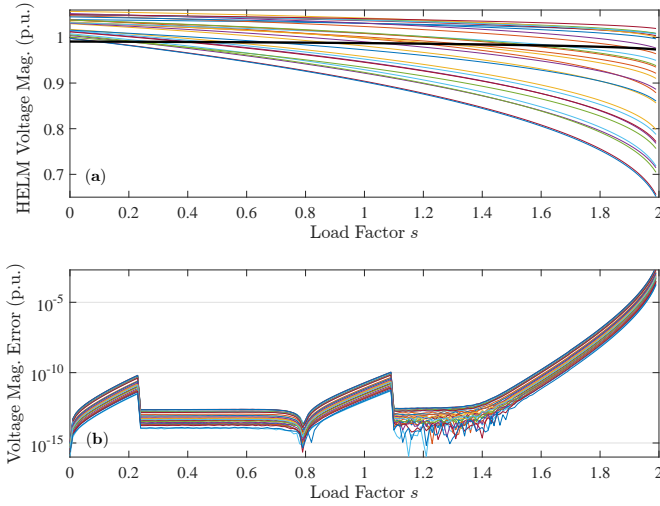


Fig. 3. Panel (a) shows the voltage magnitude for load buses of the 39 bus system as  $s$  is scaled, as computed by our adaptation of HELM; the curves in this panel are drawn analytically. The thick black curve is the voltage magnitude of bus 20, whose load is decreasing as  $s$  increases, according to equation (12). Panel (b) shows the voltage magnitude difference (error) for each PV curve between the NRPF and HELM solutions. The error is numerically insignificant until  $s$  approaches the bifurcation point ( $s \approx 2$ ).

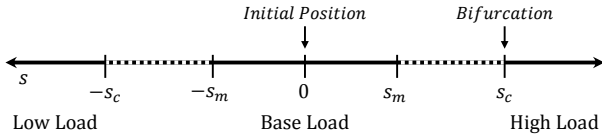


Fig. 4. An illustration of the values that the holomorphic parameter  $s$ , which starts at a base load  $s = 0$ , can attain during its random walk.  $s_m$  is the load level at which the probability of  $s$  hitting the Saddle-Node bifurcation  $s_c$  exceeds a probability limit.

$s$  as Wiener Process in which  $s$  begins at the origin and takes Gaussian-distributed steps with variance  $2D$ .

$$s[0] = 0 \quad (13)$$

$$s[k+1] = s[k] + \sqrt{2D} \cdot \mathcal{N}(1, 0) \quad (14)$$

The values which  $s$  may attain are shown in Figure 4, where  $s_c$  corresponds to a Saddle-Node bifurcation of the algebraic power flow equations. If  $s$  is allowed to drift over a time period  $t$ , and an absorbing boundary condition (the point of collapse) sits at  $s = s_c$ , the survival probability of the system, as derived in [14], is:

$$S(t) \approx \operatorname{erf} \left( \frac{s_c}{\sqrt{4Dt}} \right) \quad (15)$$

where  $\operatorname{erf}$  is the error function and  $D$  is the diffusion coefficient (based on the known variability of the load). Eq. (15) gives the probability that the parameter  $s$  will, at any point during time  $t$ , cross the voltage collapse threshold.

Additionally, we introduce the value  $s_m \in [0, s_c]$ . This scalar value corresponds to the maximum allowable load level that can be reached before the probability of voltage collapse grows too high. For example, if an operator specifies that the system must never have a collapse probability higher than

10%, then when the system reaches this probability the loading margin of the system will be  $s_c - s_m$ .

$$0.10 \approx \operatorname{erf} \left( \frac{s_c - s_m}{\sqrt{4Dt}} \right) \quad (16)$$

The connection between first passage processes and voltage collapse is further spelled out in [21]. We assume that system load changes will have both fast and slow load changes on top of some base load condition. The interaction between these fluctuations and the base load are illustrated in Fig. 5.

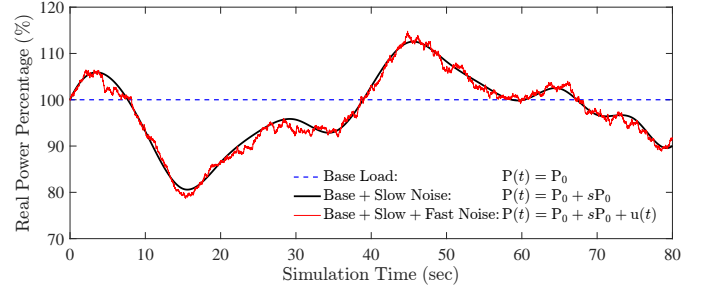


Fig. 5. The interaction between base load, the fast noise  $u(t)$  of the Ornstein-Uhlenbeck process, and the slow noise from the randomly walking Holomorphic scaling parameter  $s$  is portrayed.

### III. CONTROLLER DESIGN

This section introduces a Variance Based Controller (VBC), which is subsequently shown to successfully mitigate the probability of voltage collapse. For benchmarking and illustration purposes, we also introduce two other, more conventional, controllers: a Mean Based Controller (MBC) and a Reference Based Controller (RBC). For clarity, we introduce these controllers in reverse order of complexity (least to most). In actual implementation, both the MBC and VBC controller systems require real time (PMU) load voltage observability and a controllable reactive power resource, such as a Synchronous Condenser or a Static VAR Compensator (SVC) that can support load voltage.

#### A. Reference Based Controller Overview

The RBC does not rely on the Wide Area Measurement System (WAMS); instead, it uses a local voltage terminal measurement  $V_t$  as a feedback signal to control the reactive power injected by a “quasi-static SVC” device<sup>1</sup>. This relatively simple approach to feedback SVC control is illustrated in Fig. 6. In this diagram,  $\Delta b_{\text{SVC}}$  is the change in susceptance at the SVC and the regulator gain  $K_r$  is tuned to properly correlate voltage changes with reactive power injections. The reactive power changes are limited by the size, in MVar, of the SVC. The “BAF” block represents a Buffered Average Filter that provides a rolling average bus voltage magnitude over an operator-specified time window  $T_w$ . After  $T_w$  seconds, the BAF computes average voltages and the SVC adjusts its

<sup>1</sup>In typical power system modeling, SVC devices can be dynamically modeled with sets of ODEs. Since we are using the statistics of buffered time series data to make control decisions, we have the SVC take discrete, rather than continuous, control action every  $T_w$  (time window) seconds. We therefore refer to the device as a “quasi-static SVC”.

reactive power injection as needed. Finally, the “Network” block represents the physical feedback provided by the natural evolution of bus voltages due to control input, load fluctuations, and system dynamics.

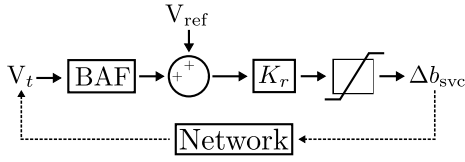


Fig. 6. Reference Based Controller (RBC). Local terminal bus voltage  $V_t$  is the only feedback signal.

### B. Mean Based Controller Overview

Similar to the Automatic Voltage Control (AVC) system outlined in [22], the MBC relies not only on local terminal voltage, but also on bus voltage magnitude data from a WAMS. These data, sampled at 30Hz, are also passed through a BAF with time window  $T_w$  and then are each subtracted from some critical magnitude  $\mu_{crit}$  and summed together. The thresholds imposed by  $\mu_{crit}$  are chosen based on minimum tolerable voltages (such as 0.98 p.u., for example); probabilistic security margins are not considered. As illustrated in Fig. 7, the voltage magnitudes  $V_1 \dots V_n$  represent WAMS data from PMUs, and the gain  $K_m$  is set based on how the operator wishes for the WAMS feedback and the local feedback to interact.

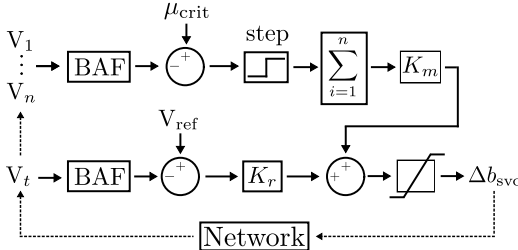


Fig. 7. Mean Based Controller (MBC). The WAMS acquire voltage magnitude data  $V_1 \dots V_n$  to use as feedback signals for the SVC.

The “step” function in Fig. 7 (and Fig. 8) operates exactly as the unit step function of equation (17). Its purpose is to ensure that only WAMS bus voltages that are lower than the critical voltage  $\mu_{crit}$  impact the feedback signal.

$$x \cdot u(x) = \begin{cases} x & x \geq 0 \\ 0 & x < 0 \end{cases} \quad (17)$$

### C. Variance Based Controller Overview

The VBC builds on the tools described in Section II in the following way. CPF via HELM is used to quickly determine how much the load within a load pocket of concern may increase before the system undergoes static voltage collapse. Next, the First Passage Process is used to determine the load level below which the probability of voltage collapse is sufficiently low. Using this loading level, the critical bus voltage variances are found by leveraging the analytical covariance matrix solver along with load noise estimation. Finally, these critical variances are used as a feedback signal to control the

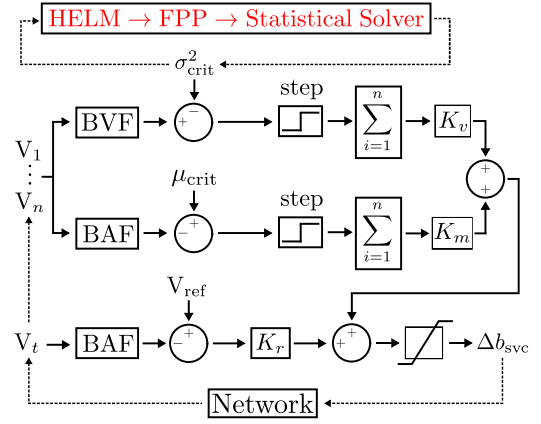


Fig. 8. Variance Based Controller (VBC). Wide Area Measurement Systems (WAMS) gather load pocket voltage magnitude data. Buffered Average Filters (BAFs) and Buffered Variance Filters (BVs) are used to quantify bus voltage magnitude and variance. The step functions ensure that **only** critically low magnitude and critically large variance measurements have effect on  $b_{SVC}$ .

reactive power injected by the quasi-static SVC device, as shown in Fig. 8.

The VBC process is formally described in Algorithm 1. The BVF, or Buffered Variance Filter, is similar to the BAF in that it computes the variance from a window of measurement data. The constant  $K_v$  is a feedback gain parameter for the variance measurements, and is tuned to allow the controller to use both the voltage magnitude and the variance feedback signals.

#### Algorithm 1: Variance Based Controller (VBC)

##### START

- 1 Perform CPF via HELM on load pocket
- 2 Determine voltage collapse loading factor  $s_c$
- 3 Based on desired probabilistic security margin, determine loading factor  $s_m$  s.t.  $0 < s_m < s_c$
- 4 Computationally scale loads based on  $s_m$  and then analytically solve for load pocket critical variance
- 5 Use critical variances and magnitude constraints as inputs to Fig. 8 controller

##### if New State Estimate Data Available then

    | Return to **START**

##### else

    | Return to **5**

##### end

## IV. 3 BUS SYSTEM ILLUSTRATION

In order to illustrate and compare the effectiveness of the controllers, we test each (RBC, MBC and VBC) on a three bus system with identical simulation parameters.

### A. System Overview

In our three-bus test case (Fig. 9), aggregate generation is connected to a heavily loaded aggregate load pocket (such as a city). The voltage magnitude of this load pocket is supported by a fully controllable quasi-static SVC, and a PMU feeds

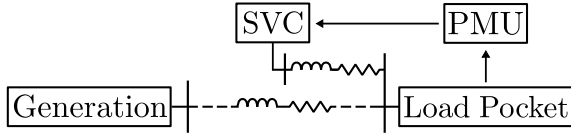


Fig. 9. 3 Bus Test Case. Aggregate generation (bus 1) feeds an aggregate load pocket (bus 2) with voltage supported by a local SVC (bus 3).

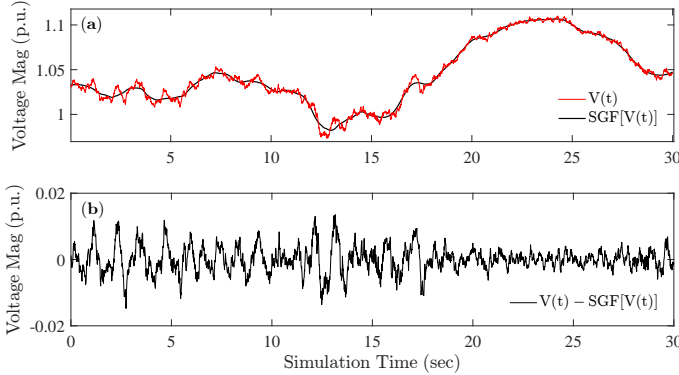


Fig. 10. Panel (a) shows a noisy time domain signal  $V(t)$  with slowly varying equilibrium changes (sped up for illustration purposes). A Savitzky-Golay Filter is applied to  $V(t)$ . In panel (b), the filtered signal is subtracted from the noisy signal in order to generate the high frequency voltage fluctuations. This difference signal is used to compute bus voltage variance.

voltage magnitude data back to the SVC in real time. (In the case of the RBC, these PMU data are neglected.)

We outfit the generator with a 4<sup>th</sup> order Synchronous Machine (SM), a 4<sup>th</sup> order Automatic Voltage Regulator (AVR), and a 3<sup>rd</sup> order Turbine Governor (TG). System parameters are approximately based on the WSCC 9-bus system, and component models are those described in [16]. At the SVC, we choose a buffering time window of  $T_w = 3$ s. The load of the load pocket is constant power (PQ); the fast load fluctuations are described by the Ornstein-Uhlenbeck process of (5) and the slow load variations are monotonically increased (see panel (b) of Fig. 11). Both fast and slow load fluctuations were applied to the active and reactive power demands equally in order to hold power factor constant.

To compare the three controllers, we (i) initialized the heavily loaded 3 bus system, (ii) performed a time domain simulation with a stochastically increasing load, and (iii) measured the survival time achieved by each controller. Fast Ornstein-Uhlenbeck noise is applied at each integration time step of  $\Delta t = 0.01$ . For each simulation, we record the random fast and slow noise vectors applied to the loads such that each controller experiences identical simulation realizations.

In order to estimate the high frequency variance  $\sigma^2$  of a voltage signal whose underlying equilibrium point is constantly shifting due to the slow load fluctuations the real-time measurements must first be detrended. To do so, we employ a 2<sup>nd</sup> order FIR Savitzky-Golay Filter (SGF) to the voltage time series data and then subtract the smoothed voltage signal from the original data. This yields the zero-mean high frequency voltage perturbations, as illustrated in Fig. 10.

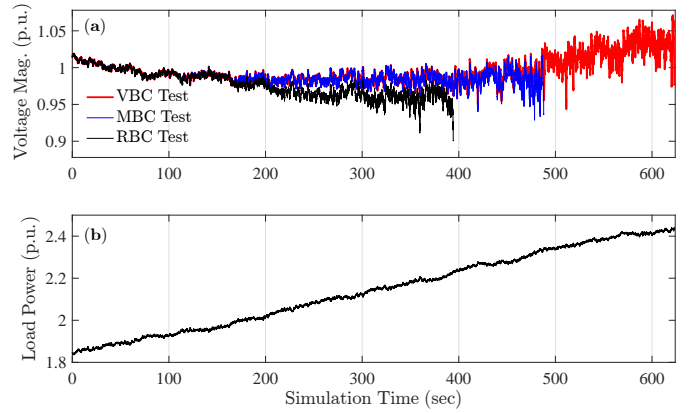


Fig. 11. Panel (a) shows the load bus voltage magnitude over the span of the simulations associated with all three controllers up to the point of voltage collapse. Panel (b) shows the active power demand at the load bus (identical for all three simulations).

## B. Simulation Results

With each controller, we simulated the system up until the point of voltage collapse. As previously indicated, the fast and slow noise vectors for the simulation were computed and saved before running each simulation, such that each controller experienced an identical simulation case. Table I summarizes two primary test results: the amount of time each controller kept the system “alive” (prevented bifurcation) and the amount of load increase that the system was able to sustain. Clearly, the Variance Based Controller most effectively preserved voltage stability while load increased.

TABLE I  
SIMULATION RESULTS SUMMARY

Test Result	RBC	MBC	VBC
Bifurcation Time (sec)	394.26	487.87	623.05
Bifurcation Load Increase (%)	21.2%	27.0%	32.8%

To further illustrate these results, Fig. 11 shows the load bus voltage magnitude over time (panel (a)) for all three controllers until the point of bifurcation and the active power demand (panel (b)) at the load bus.

The results in Fig. 11 show that all three controllers take identical action until roughly 200 seconds. At this point, the WAMS feedback signal of the remote load bus voltage begins to drop low enough to warrant control action. The RBC simulation bifurcates at around 400 seconds, but the MBC is able to maintain stability until about 490 seconds. At this point, the VBC begins to take control action due to the extreme increases in the bus voltage variance. Since it relies only on bus voltage magnitude data, the MBC is unaware that additional control action is needed and fails to maintain stability.

In Fig. 12, the bus voltage variance crosses the “critical” threshold just before  $t = 400$ . The VBC simulation begins to call for increasing SVC support and thus prevents the system from bifurcating at  $t = 490$ , when the MBC system fails. As can be inferred from Fig. 2 and equation (1), the bus voltage variance begins to show an exponential increase when the system load approaches the stability limit. As a result,



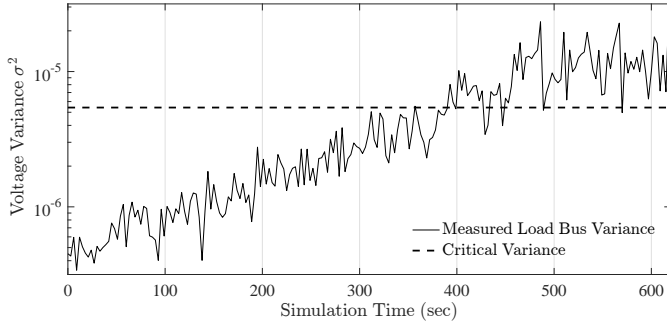


Fig. 12. The discretely measured (every  $T_w = 3$  seconds) load bus voltage variance is plotted over the simulation lifespan for the VBC.

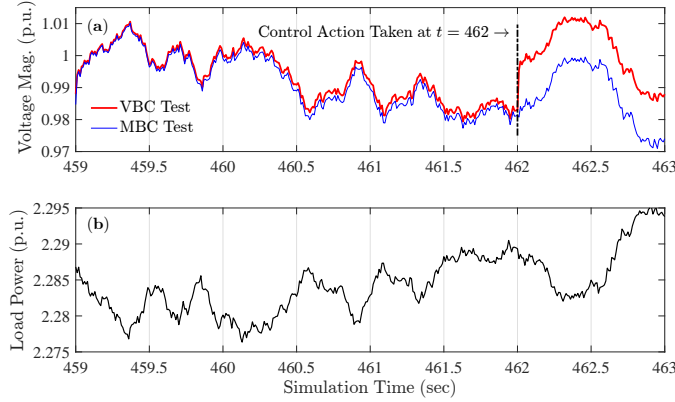


Fig. 13. Panel (a) show the load bus voltage over a period of four seconds for two controllers, where both controllers taken control action at  $t = 462$  based on measurements taken over the time window of  $t = 459$  to  $t = 462$ . Panel (b) shows the associated active power demand at the load bus.

the control signal associated with the bus voltage variance,  $K_v(\sigma_{\text{meas}}^2 - \sigma_{\text{crit}}^2)$ , also begins to increase exponentially. This explains the upward trend of the bus voltage magnitude for the VBC test during the last 100 seconds of simulation (seen in panel (a) of Fig. 11).

It is helpful to consider a critical point when the VBC and the MBC take very different control actions. To do so, Fig. 13 zooms in on Fig. 11 to the window of time from  $t = 459$  to  $t = 463$ . In panel (b) of Fig. 13, the load fluctuations from  $t = 459$  to  $t = 462$  spike downwards despite a slow upward trend. Since the system is operating close to the stability limit at this point, bus voltages spike high, above 1 per unit. Therefore, since the mean voltage over the time window from  $t = 459$  to  $t = 462$  appears relatively high, the MBC takes almost no control action. The VBC, on the other hand, measures an extremely high bus voltage variance and thus takes strong control action, despite the relatively high mean voltage magnitude (which is above 0.99 p.u.). This is but one of many examples of the VBC taking control action when the MBC does not. As more and more SVC support is added to the system, the mean voltage magnitude becomes an unreliable signal for system voltage health as the bifurcation voltage drifts closer to nominal system voltage. Bus voltage variance, on the other hand, is a robust indicator of a system's proximity to voltage collapse.

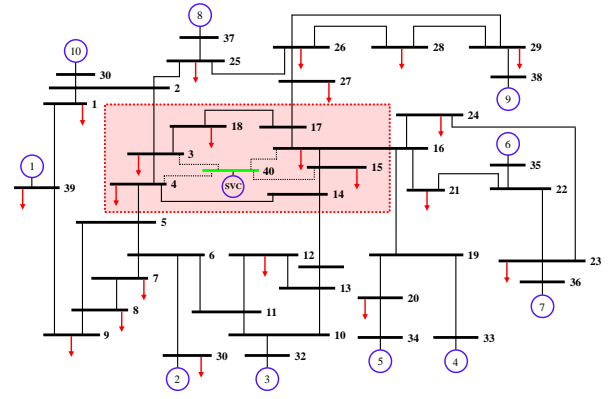


Fig. 14. IEEE 39 bus system with added SVC Bus.

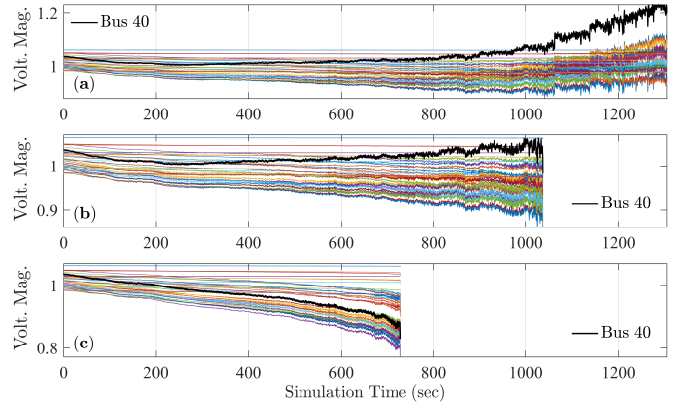


Fig. 15. Bus voltage magnitudes from simulations of the 39 bus test case with three different control systems, as load increases up until the point of voltage collapse. Panel (a) shows results from the VBC, panel (b) shows results from MBC, and panel (c) includes results for RBC. In each panel, the SVC bus voltage (bus 40) is noted.

## V. 39 BUS SYSTEM TEST RESULTS

For further validation, we tested the controllers on a modified version of the IEEE 39 bus system. As shown in Fig. 14, an SVC bus (bus “40”) was added to the system and connected to 4 other buses to form an observable (via PMU) load pocket with reactive support. To test the controllers in this system, monotonically increasing slow load changes were applied to all load pocket buses (3, 4, 14, 15, 16, 17, and 18), in addition to fast mean reverting Ornstein-Uhlenbeck load noise. As with the three-bus results in Fig. 11, the results clearly illustrate that the Variance Based Controller improves voltage stability most effectively, relative to the reference controllers.

Fig. 15 shows the voltage evolution for the tests corresponding with all three controllers. The VBC deters voltage collapse 270 seconds longer than the MBC and 579 second longer than the RBC. To better understand the success of the VBC, Fig. 16 shows the bus voltage variance and the average critical voltage variance. Since each bus has a unique critical voltage variance, as computed by (II-C), for the sake of graphical clarity, only the average critical variance is shown.

Because the VBC measures the differences between the measured and critical variances, and then scales these values by  $K_v$  and sums them across buses, large increases in variance

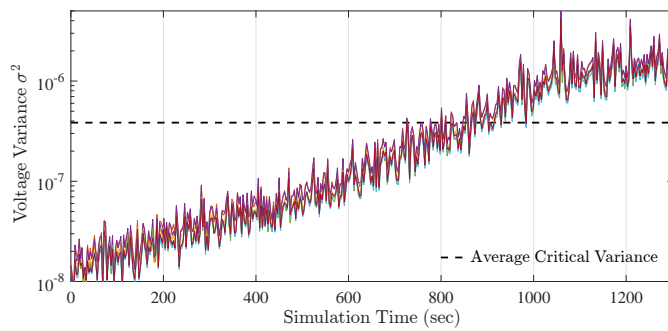


Fig. 16. Bus voltage variance in the 39 bus test case, as load increases over time.

(which are expected as a system approaches its stability limit) lead to very large reactive power injections, even when voltage magnitude remains relatively “high”. These variance increases are clearly seen in Fig. 16.

## VI. CONCLUSION

In this paper, we introduce and provide test results for a new reactive power control system that uses bus voltage variance as a control signal to improve voltage stability. Tests of this system on a three-bus test case show that the Variance Based Controller (VBC) can maintain voltage stability if load increases to 32.8% above nominal, whereas a Mean Based Controller (MBC) allows for a load increase of only 27.0% above nominal, and the Reference Based Control (RBC) allows for a load increase of only 21.2%. Tests of the new control system on the 39 bus test case, in which load was steadily increasing, show that the VBC deterred voltage collapse 270 and 579 seconds longer than the MBC and RBC, respectively. Both sets of results clearly show that statistical information can be valuable in reducing the risk of voltage collapse.

Future work aims to extend the validation to understand how the VBC functions in a larger system with more realistic load profiles. Similarly, future work could extend the variance-based controller to include other types of statistical warning signs, such as autocorrelation.

## REFERENCES

- [1] I. Dobson, B. a. Carreras, V. E. Lynch, and D. E. Newman, “Complex systems analysis of series of blackouts: Cascading failure, critical points, and self-organization,” *Chaos*, vol. 17, 2007.
- [2] T. Ohno and S. Imai, “The 1987 tokyo blackout,” in *Power Systems Conference and Exposition, 2006. PSCE '06. 2006 IEEE PES*, pp. 314–318, Oct 2006.
- [3] M. Scheffer, J. Bascompte, W. a. Brock, V. Brovkin, S. R. Carpenter, V. Dakos, H. Held, E. H. van Nes, M. Rietkerk, and G. Sugihara, “Early-warning signals for critical transitions,” *Nature*, vol. 461, 2009.
- [4] C. Wissel, “A universal law of the characteristic return time near thresholds,” *Oecologia*, vol. 65, no. 1, pp. 101–107, 1984.
- [5] V. Dakos, E. H. Van Nes, P. D’Odorico, and M. Scheffer, “Robustness of variance and autocorrelation as indicators of critical slowing down,” *Ecology*, vol. 93, 2012.
- [6] G. Ghanavati, P. D. H. Hines, T. I. Lakoba, and E. Cotilla-Sanchez, “Understanding early indicators of critical transitions in power systems from autocorrelation functions,” *IEEE Transactions on Circuits and Systems I: Regular Papers*, vol. 61, Sep. 2014.
- [7] D. Podolsky and K. Turitsyn, “Random load fluctuations and collapse probability of a power system operating near codimension 1 saddle-node bifurcation,” in *IEEE Power and Energy Soc. Gen. Meeting*, Jul. 2013.

- [8] E. Cotilla-Sanchez, P. Hines, and C. Danforth, “Predicting critical transitions from time series synchrophasor data,” *IEEE Transactions on Smart Grid*, vol. 3, pp. 1832–1840, Dec. 2012.
- [9] G. Ghanavati, P. D. H. Hines, and T. I. Lakoba, “Identifying useful statistical indicators of proximity to instability in stochastic power systems,” *IEEE Transactions on Power Systems*, vol. (in press), 2015.
- [10] R. Sodhi, S. C. Srivastava, and S. N. Singh, “A simple scheme for wide area detection of impending voltage instability,” *IEEE Transactions on Smart Grid*, vol. 3, pp. 818–827, June 2012.
- [11] A. A. P. Lerm, C. A. Canizares, and A. S. e Silva, “Multiparameter bifurcation analysis of the south brazilian power system,” *IEEE Transactions on Power Systems*, vol. 18, May 2003.
- [12] P. Kundur, J. Paserba, V. Ajarapu, et al., “Definition and Classification of Power System Stability,” *IEEE Transactions on Power Systems*, vol. 21, no. 3, pp. 1387–1401, 2004.
- [13] A. Trias, “The holomorphic embedding load flow method,” in *2012 IEEE Power and Energy Society General Meeting*, July 2012.
- [14] S. Redner, *A Guide to First-Passage Processes*. Cambridge University Press, 2001. Cambridge Books Online.
- [15] S. Greene, I. Dobson, and F. L. Alvarado, “Sensitivity of the loading margin to voltage collapse with respect to arbitrary parameters,” *IEEE Transactions on Power Systems*, vol. 12, pp. 262–272, Feb 1997.
- [16] F. Milano, *Power System Analysis Toolbox Reference Manual for PSAT version 2.1.6.*, 2.1.6 ed., 5 2010.
- [17] C. W. Gardiner, *Handbook of Stochastic Methods for Physics, Chemistry, and the Natural Sciences*. Berlin, Germany: Springer, 4th ed., 2004, Sec. 4.4.6, pp. 109–112.
- [18] V. Ajarapu and C. Christy, “The continuation power flow: a tool for steady state voltage stability analysis,” *IEEE Transactions on Power Systems*, vol. 7, pp. 416–423, Feb 1992.
- [19] S. Rao, Y. Feng, D. J. Tylavsky, and M. K. Subramanian, “The holomorphic embedding method applied to the power-flow problem,” *IEEE Transactions on Power Systems*, vol. PP, no. 99, 2015.
- [20] M. Subramanian, “Application of holomorphic embedding to the power-flow problem,” Master’s thesis, Arizona State University, July 2015.
- [21] S. Chevalier, “Using real time statistical data to improve long term voltage stability in stochastic power systems,” Master’s thesis, University of Vermont, October 2016.
- [22] Z. Liu and M. D. Ili, “Toward pmu-based robust automatic voltage control (avc) and automatic flow control (afc),” in *IEEE PES General Meeting*, pp. 1–8, July 2010.



**Samuel C. Chevalier** (S’13) received M.S. (2016) and B.S. (2015) degrees in Electrical Engineering from the University of Vermont, and he is currently pursuing the Ph.D. in Mechanical Engineering from MIT. His research interests include stochastic power system stability, renewable energy penetration, and Smart Grid applications.



**Paul D. Hines** (S’96, M’07, SM’14) received the Ph.D. in Engineering and Public Policy from Carnegie Mellon University in 2007 and M.S. (2001) and B.S. (1997) degrees in Electrical Engineering from the University of Washington and Seattle Pacific University, respectively. He is currently an Associate Professor in the Dept. of Electrical and Biomedical Engineering, with a secondary appointment in the Dept. of Computer Science, at the University of Vermont. He also serves as the vice-chair of the IEEE PES Working Group on Cascading

Failures and is a co-founder of Packetized Energy, a distributed energy software company.